UNIVERSITÀ DI PARMA

UNIVERSITA' DEGLI STUDI DI PARMA

DOTTORATO DI RICERCA IN

" *Scienze Mediche e Chirurgiche Traslazionali*"

Ciclo XXVII

"Simplified Extraprostatic Extension grade (sEPE grade): a new predictive score for MRI assessment of extraprostatic tumor extension"

Coordinatore:

Chiar.mo Prof: **N.Sverzellati**

Tutor:

Chiar.mo Prof: **N.Sverzellati**

Dottorando: **Silvia Schirò**

Anni Accademici 2021/2022-2023/2024

Simplified Extraprostatic Extension grade (sEPE grade): a new predictive score for MRI assessment of extraprostatic tumor extension

Abstract

Objectives: (i) to assess the reproducibility and predictive value of a simplified score for evaluating extraprostatic tumor extension (sEPE grade). (ii) To test the predictive value of the simplified score on site specific tumor location namely anterior or posterior zone.

Methods: Sixty-five patients (mean age ± SD, 67 years±6.3) with prostate cancer treated by radical prostatectomy, who underwent 1.5 Tesla multiparametric magnetic resonance imaging (mpMRI) within six months before surgery, were included. Concerning tumor location: in 18 patients' prostate cancer was in the anterior zone and in 42 patients was in the posterior zone. sEPE grade was derived from mpMRI metrics: curvilinear contact length >15 mm (CCL), and capsular bulging/irregularity. The diameter of the index lesion (dIL) was also measured. Evaluations were independently performed by seven radiologists, and inter-reader agreement was tested by weighted Cohen K coefficient. A nested (two levels) Monte Carlo cross-validation was used. The best cut-off value for dIL was selected by means of the Youden J index to classify values into a binary variable termed dIL*. Logistic regression models based on sEPE grade, dIL* and clinical scores were used to predict pathologic EPE. Results on validation set were assessed by the main metrics of the Receiver Operating Characteristics Curve (ROC). Decision curve analysis (DCA) was performed. Based on our findings we defined and tested an alternative sEPE grade formulation.

Afterwards, the diagnostic performance of the alternative sEPE grade formulation was assessed on site specific tumor location.

Results: Pathologic EPE was identified in 31/65 (48%) patients. The average weighted kappa coefficient was 0.65 (95%C.I. 0.51-0.79), 0.66 (95%C.I. 0.48-0.84), 0. 67 (95%C.I. 0.50-0.84), and 0.43 (95%C.I. 0.22-0.63) for sEPE grading, CLL ≥15 mm, dIL* and capsular bulging/irregularity, respectively. The highest diagnostic yield in predicting EPE was obtained by combining both sEPE grade and dIL*(ROC-AUC 0.81). sEPE showed the highest AUC of 88% for depicting EPE of the anterior zone lesions.

Conclusions: The sEPE grade is reproducible and, when combined with dIL*, effectively predicts extraprostatic tumor extension, especially for anterior zone lesions.

Keywords: prostatic neoplasms; diagnostic imaging; multiparametric magnetic resonance imaging; neoplasm grading.

Introduction

Prostate Cancer

Prostate cancer is a major global health challenge, ranking amid the top five cancers for incidence and mortality [1]. It is the second most common malignancy in males, characterized by striking geographical variation in both incidence and mortality rates.

Prostate cancer is more prevalnt in developed countries. By age 79 years, the odds of being diagnosed with prostate cancer is about one in 47 among countries with a low-middle sociodemographic index, comparted with one in six in countries with high sociodemographic index [2].

Incidence

Notably, the global variation of prostate cancer incidence it's significant. For istance, African-American men in the United States have some of the highest age-adjusted incidence rates, while Asian men living in their native countries have some of the lowest [3]. Part of this difference, can be explained by how intensively prostate-specific antigen (PSA) screening is used in different regions. However, the fact that prostate cancer rates varied even before PSA screening was widely introduced suggests that lifestyle factors also play a role in shaping disease risk, with significant morbidity and mortality rates [4].

Mortality

Prostate cancer ranks as he fifth leading cause of cancer-related deaths worldwide, responsible for an estimated 366,000 deaths [2]. While prostate cancer is more commonly diagnosed ion developed regions, mortality rates are actually higher in less developed areas, highlighting a

difference between incidence and outcomes across the globe. A recent review of Culp et al. [5] showed incidence and mortality trends worldwide. Concerning Southern-Europe, Slovenia, had the highest prostate cancer incidence rates among the six nations studied, followed by Spain. On the other hand, prostate cancer incidence trends have declined in Italy and stabilized in the remaining countries. Regarding mortality rate, both Greece and Italy have seen a decline, while the other countries have experiences stable mortality rates [5].

The changes in mortality rates are due to a combination of factors, including the incidence and survival among patients.

Risk factors

Epidemiologic studies of prostate cancer have shown that both individual biology and lifestyle factors effect risk of developing the disease as well as their chances of survival. Given the clinical heterogenicity of prostate cancer is it instrumental to differentiate between risk factors for prostate cancer and for advanced/fatal disease.

Risk factors may affect prostate cancer throughout its progression, from the initial development of the disease to its spread and, ultimately, to the exitus. It's likely that the risk factors for prostate cancer would differ from those that contribute to a more aggressive form of the disease.

The evidence of the following risk factors older age, African descent, family history, genetic risk loci is strong for prostate cancer.

Prostate cancer is rare among men younger than forty years of age. The incidence rate rises significantly after the age fifty-five year, a pattern seen worldwide in both low-and highly developed countries. There are also noticeable differences in prostate cancer incidence and

mortality among various racial and ethnic groups. For instance, in the United States black men showed the highest incidence. Genetic risk loci across racial/ethnic group could account for some differences in incidence rates [6]. Having a family history of prostate cancer increases a man's risk of developing the disease. Men with a father or brother who has been diagnosed are at higher risk, and that risk is even higher for those who have both father and brother with prostate cancer [7]. A similar trend is observed when it comes to the risk of lethal prostate cancer. Men with a first-degree relative who died from prostate cancer are at greater risk of dying from the disease themselves, compared to those who have neem diagnosed with prostate cancer without a family history. More than a hundred of risk loci confirmed across multiple studies have been found. A recent study of Haiman et al [6] showed that the risk region at 8q24 was the strongest predisposition locus for prostate cancer in different populations.

Risk factors strongly associated with advanced or lethal prostate cancer are taller height, obesity and smoking. On the other hand, the only risk factor strongly associated with decreased risk of advanced or fatal disease is physical activity [1].

Concerning obesity, itself a global health issue affecting 11% of adults worldwide, it disrupts hormonal pathways leading to increase insulin levels and inflammation factors and decrease testosterone and sex hormone binding protein [8, 9]. Obesity is associated with increased risk of prostate cancer mortality and recurrence. Waist circumference an index of abdominal obesity, is likewise positively associated with risk of advanced prostate cancer [10].

Taller height has been proved to be strongly associated with advanced/fatal prostate cancer. Zuccolo et al [11] showed that higher risk of advance prostate cancer per 10 cm of height. A

possible explanation for this association was that height achieved in adult life reflects early life exposure to growth hormones such as insulin-like growth factor 1.

The risk of death and the risk of and advanced-stage disease is increased by smoking. Kenfield et al. have showed that compared to men who never smoked, current smokers showed 60% higher risk of prostate cancer mortality [12]. Smoking may affect prostate cancer mortality by negatively influencing response to treatment. The mechanism associated between smoking and prostate cancer risk likewise and mortality remains unclear. Several hypothesis have been suggested, such as the role of carcinogens contained in tobacco smoke that may promote tumors, alterations in testosterone levels, and various epigenetic and nicotine-related effects [12].

Physical activity was found to be the only factor with moderate inverse association with advanced/fatal cancer. Men who performed vigorous physical activity has lower risk of aggressive prostate cancer and lower risk of mortality [13, 14].

Screening and Diagnosis of Prostate Cancer

To date, there is not a specific test for prostate cancer. Screening typically involves a clinical evaluation and blood testing. A digital rectal examination provides information about the size and the texture of the prostate gland. Additionally, prostate-specific antigen (PSA) test remains instrumental for prostate cancer screening. PSA is a glycoprotein produced by the epithelial cells of the prostate and is normally found in semen, though small amounts can also enter the bloodstream [4]. The standard PSA threshold for concern is 4 ng/mL; PSA is specific to the prostate gland but not exclusive to prostate cancer; this means that elevated PSA levels can indicate benign pathologies such as benign prostatic hyperplasia and prostatitis. If the PSA

levels is more than 10 ng/mL the probability of cancer is over 50% [4]. Therefore, the need for further diagnostic tests to rule out prostate cancer or other condition is instrumental.

Multiparametric MRI in Prostate Cancer Staging

mpMRI combines multiple MRI sequences to provide a comprehensive evaluation of prostate cancer. Prostate imagint at 3 Tesla benefits of higher signal to noise ratio, however is not commonly performed in clinical practice in Italy. Use of endorectal coil is not an absolute requirement for cancer detection protocol [15]. The standard mpMRI protocol typically includes T2-weighted imaging (T2-WI), diffusion-weighted imaging (DWI), and dynamic contrast-enhanced imaging (DCE). Each sequence contributes unique diagnostic information:

1. **T2-Weighted Imaging (T2-WI)**:

   T2-WI provides high spatial resolution and excellent soft-tissue contrast, making it the gold standard for anatomical assessment of the prostate gland. It is particularly useful for visualizing the prostatic capsule, neurovascular bundles, and seminal vesicles.

2. **Diffusion-Weighted Imaging (DWI)**:

   DWI assesses the diffusion of water molecules within tissues and provides functional information about tumor cellularity. Prostate cancer typically exhibits restricted diffusion due to its dense cellular structure, which appears as hyperintensity on DWI and hypointensity on the apparent diffusion coefficient (ADC) map. DWI is particularly useful for detecting and characterizing prostate tumors, especially in the peripheral zone

3. **Dynamic Contrast-Enhanced Imaging (DCE)**:

   DCE evaluates the vascularity of prostate tissues by monitoring the uptake and washout

of gadolinium-based contrast agents. Prostate cancer tends to show early and rapid contrast enhancement compared to normal tissues, reflecting increased angiogenesis.

When mpMRI is indicated?

A recent review [15], described three main role for mpMRI: (i) in biospy naïve patients, (ii) following biopsy and (iii) in active survellaince.

(i) The use of multiparametric MRI (mpMRI) in biopsy-naïve patients may be cost-effective, as it can lead to a reduction in overdiagnosis and overtreatment when performed prior to biopsy [16]. Furthermore, mpMRI has been shown to enhance biopsy performance and improve the detection of clinically significant tumors [17].

(ii) mp-MRI demonstrates significant potential in detecting clinically relevant prostate cancers, particularly in patients with previous negative biopsies. A meta-analysis indicates a cancer detection rate of 37.5%, with high specificity (90%) and varying positive predictive values [15]. Studies highlighted that targeted biopsies guided by mp-MRI can identify additional significant cancers not detected by systematic biopsies, underscoring mp-MRI's role in improving diagnostic accuracy and patient outcomes.

(iii) Mp-MRI showed a sensitivity of 93%, a positive predictive value of 57%, and an overall accuracy of 92%. These results suggests that mp-MRI could by a very helpful in choosing the right treatment options, whether for active surveillance or radical treatment. For men with low-risk disease, not having a visible lesion on mp-MRI might be a positive sign, as it could lead to fewer unnecessary biopsy procedure. reduce the number of unnecessary biopsy procedures. Using mpMRI as a

surveillance tool in place of biopsies for detecting clinically significant cancer shows promise.

Prostate MRI anatomy

Zonal Anatomy

The transition zone surrounds the prostatic urethra and tends to enlarge in older men, leading to benign prostatic hyperplasia. The central zone, located at the base of the prostate behind the transition zone, surrounds the left and right ejaculatory duct. On the front site of the prostate, there's a small area called the anterior fibromuscular. The peripheral zone is found on the back and lateral side of the prostate (**Figure 1**).

Figure 1. Graphic representation of zonal anatomy and most common origin of prostate cancer

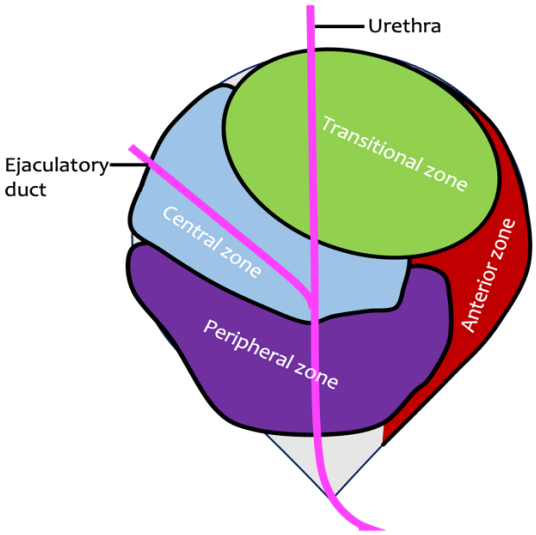

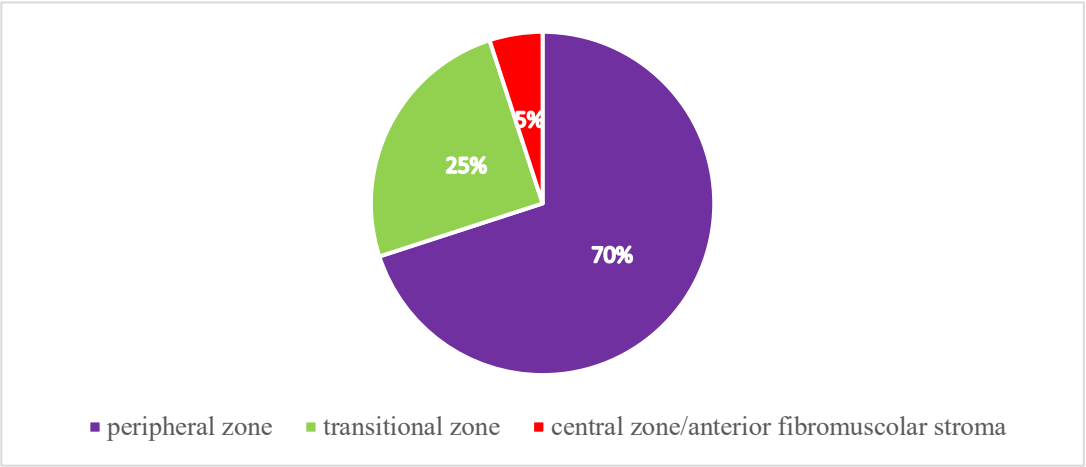

PI-RADS

The Prostate Imaging Reporting and Data system (PI-RADS) defined standards of high-quality clinical services for mp-MRI including image acquisition and reporting. PI-RADS aims at assessing the risk of clinically significant prostate cancer. The to date version is v.2.1. PI-RADS assessment category for each lesion is based on the scoring of T2-weighted, DWI/ADC and DCE sequences according to zonal anatomy. For the peripheral zone the DWI/ADC is the primary

determining sequence to assign PI-RADS assessment category. For the transition zone the T2W images is the primary determining sequence to assign the PI-RADS assessment category. Peripheral zone PI-RADS is shown in **Table 1** and transition zone is shown in **Table 2**.

Table 1. PI-RADS of the peripheral zone

	1	Catergory 1 • No abnormality visible on ADC and high b-value of DWI.
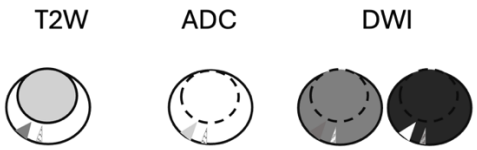	2	Category 2 • Linear/wedge shaped configuration with hypointensities on ADC and/or linear/wedge shaped hyperintensities on high b-value DWI
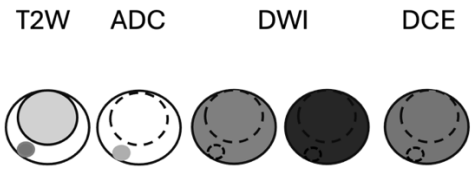	3	Category 3 • Focal (discrete and different from the background) hypointensity on ADC and/or focal hyperintensity on high 3 b-value DWI • May be markedly hypointensity on ADC or markedly hyperintensity on high b-value DWI but not both • No focal enhancement on DCE
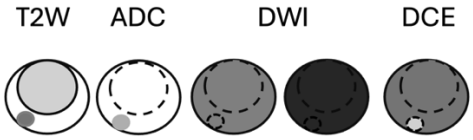	4	Category 4 • Focal (discrete and different from the background) hypointensity on ADC and/or focal hyperintensity on high 3 b-value DWI • May be markedly hypointensity on ADC or markedly hyperintensity on high b-value DWI but not both • Focal enhancement on DCE
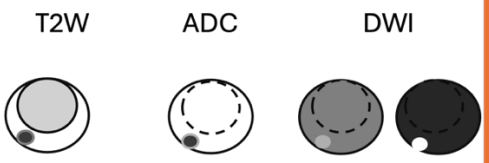	4	Category 4 • Focal marked hypointensity on ADC and marke hyperintensity on high b-value DWI • <1.5 cm in greatest dimension
	5	Category 5 • Same assessment score 4 but ≥ 1.5 cm in greatest dimemsion or • Definite extraprostatic extension (EPE) or invasive behaviour

**DWI two values of b- grey b-800/1000 and dark grey b-1400/200*

Table 2. PI-RADS of the Transition zone

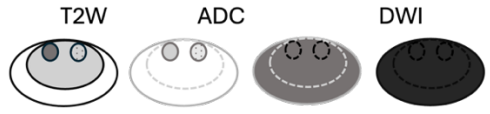	1	Catergory 1 • Normal appearing of TZ (rare) or • Round completely encapsulated nodule ("Typical nodule")
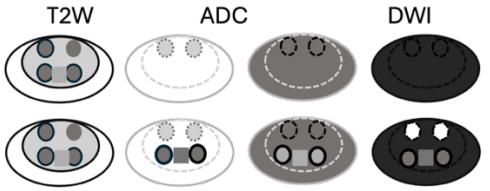	2	Category 2 • Mostly encapsulated nodule • Homogeneous circumscribed nodule without encapsulation ("atypical nodule) or • Homogenous mildly hypointesne area between nodules • DWI ≤ 3
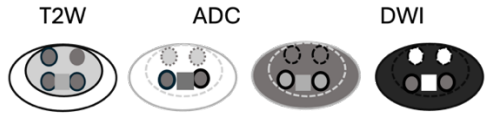	3	Category 3 • Like category 3 • If the DWI has a score of 4 or more
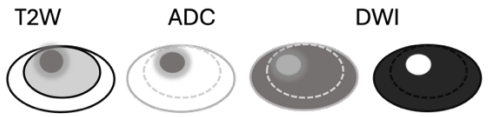	3	Category 3 • Heterogeneous signal intensity with obscured margins • Includes other that do not qualify as 2,4, or 5 • the DWI has a score ≤ of 4
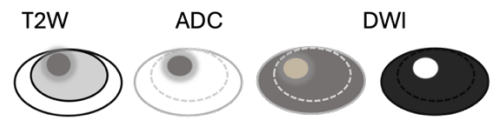	4	Category 4 • Like catergory 3 • The DWI has a score of 5
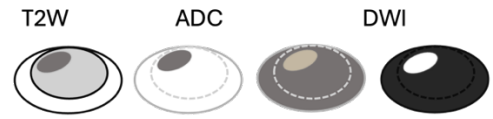	4	Category 4 • Lenticular of non-circumscribed,homogeneous, moderately hypointense • And < 1.5 cm in greates dimenion
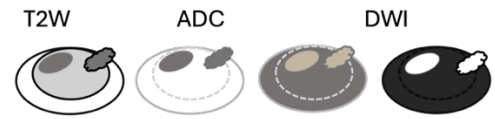	5	Category 5 • Same assessment score 4 but ≥ 1.5 cm in greatest dimemsion or • Definite extraprostatic extension (EPE) or invasive behaviour

**DWI two values of b-grey b-800/1000 and dark grey b-1400/200*

Risk stratification

The diagnosis of prostate cancer involves microscopic examination of prostate tissue obtained through a needle biopsy. Typically, a systematic prostate biopsy is conducted using transrectal ultrasound, which allows for the collection of 10 to 12 tissue samples in a grid pattern [3]. A pathologist the analyses these samples and assigns a primary Gleason grade to the common

predominant histological pattern and a secondary grade for the next highest pattern, both rated on a scale of 1 to 5 based on the cell's microscopic structed and appearance [3]. Clinicians use the Gleason scores, along with PSA levels and clinical stage, to categorize the diagnosis into low, intermediate or high (**Table 3**).

Table 3. Risks stratification Schema for Prostate Cancer

National Comprehensive Cancer Network Risk Stratification	
Very low risk	Clinical stage of T1c, Gleason score of 6 or less, PSA level less than 10 ng/mL, less than 3 biopsy cores with cancer presence of 50% or less in each core and PSA density of less than 0.15 ng/mL/g
Low risk	Clinical stage of T1 to T2a, Gleason score of 6 or less, and PSA level of less than 10 ng/mL
Intermediated risk	Clinical stage of T2b to T2c, Gleason score of 7, PSA level of 10 to 20 ng/mL
High risk	Clinical stage of T3a, Gleason score of 8 to 10 or PSA level greater than 20 ng/mL
Very high risk	Clinical stage of T3b to T4, primary Gleason score pattern 5 or greater than 4 biopsy cores with Gleason score of 8 to 10
Prostate cancer Nomograms	
Calculate probability (0%-100%) of extent disease, biochemical recurrence, cancer specific survival based on age, PSA level, clinical stage, Gleason score, percentage of biopsy cores involved with cancer	
Cancer of the Prostate Risk Assessment	
Scoring system from 0 to 10 based on age, PSA level, Gleason pattern 4 or 5, clinical stage, percentage of biopsy cores involved with cancer	
	Low risk score: 0-2
	Intermediate risk score: 3-5
	High risk score: 6-10
Pathologic Grading System of the International Society of Urological Pathology	
Grade 1 cancer: Gleason score of 3+3	
	Only individual, discrete, well-formed gland
Grade 2 cancer: Gleason score of 3+4	
	Predominantly well-formed gland with lesser component of poorly formed, fused or cribiform glands
Grade 3 cancer: Gleason score 4+3	
	Predominantly poorly formed, fused or cribiform glands with lesser component of well-formed glands
Grade 4 cancer: Gleason scores 4+4, 3+5 and 5+3	
	Only poorly formed, fused or cribiform gland or well-formed glands plus area of lacking glands
Grade 5 cancer: Gleason scores 4+5, 5+4 and 5+5+	
	Lacks gland formation (or with necrosis) with or without poorly formed, fused or cribiform gland.

Risk stratification depends on a precise prostate biopsy. Even though systematic prostate biopsy remains the standard of care, this approach misses 21%-28% of prostate cancers and

undergrads 14-17% [3]. Among the various new biomarkers developed to help identify potential false negatives, prostate cancer antigen 3 (PCA3) test stands out particularly promising. Patients who receive a normal result of PCA3 test have an 88% likelihood of negative prostate biopsy, indicating a strong predictive value in ruling out prostate cancer.

Recent advancements in imaging technology have improved diagnostic capabilities, with multiparametric MRI (mpMRI) being particularly significant. MRI demonstrated a pooled sensitivity of 89% and specificity of 73% in detecting prostate cancer [3]. There are three main methods for obtaining targeted biopsies of suspicious lesions: (i) fusing MRI images with transrectal ultrasound through specialized software, (ii) performing a percutaneous biopsy while the patient is undergoing MRI, and (iii) visually reviewing the MRI before conduction a sequential prostate biopsy with transrectal ultrasound.

A large prospective study proved that the targeted prostate biopsy using MRI-ultrasound fusion identified 30% more cases of clinically significant prostate cancer compared to traditional systematic biopsies[3].

The advent of minimally invasive surgical techniques, such as laparoscopic and robotic prostatectomy, has also led to improved functional outcomes of patients undergoing radical surgery [18, 19]. Therefore, a precise pre-operative staging and risk stratification are crucial for nselecting the most appropriate treatment options [20].

Extraprostatic extension

Tumor extent beyond prostate capsule (extraprostatic extension, EPE) might preclude radical treatments, with unfavorable effect on prognosis [20]. The presence of EPE compels wider excision margins, and is associated with higher rates of biochemical recurrence, metastatic

disease, and lower survival rates [21, 22]. To overcome the higher risk of postoperative erectile dysfunction and/or urinary incontinence associated with radical prostectomy (PR), nerve-sparing RP (NSRP) may be considered in patients with low-risk prostate cancer [23-25]. Notably, suitability for NSRP is closely impacted by EPE [26]. Therefore, an appropriate evaluation of EPE prior to surgery may be a factor in planning surgical strategies, providing the best oncologic outcome with a minimal impact on the quality of life.

mpMRI can accurately stage prostate cancer, although with low sensitivity for EPE (about 60%) [27-29]. Seminal vesicles invasion, neurovascular asymmetry, frank capsular breach, obliteration of the rectoprostatic angle, capsular bulge and broad capsular contact are morphologic predictors of EPE at MRI [30]. Quantitative measurements such as the "length of capsular contact" or the "size of the index lesion" [31] were likewise tested for assessing EPE [31-36], showing higher rates of reproducibility as compared to qualitative approaches [28, 37, 38]. To reduce variability in EPE assessment, an EPE grading method including quantitative and qualitative metrics was proposed, with high level of accuracy [26, 39]. Among the evaluated metrics, the highest inter-observer agreement was described for "curvilinear contact length" (CCL) and "capsular bulging/irregularity", although the other tested metrics were affected by lower inter-observer agreement [26].

Key MRI Features of EPE

Several radiological signs on mpMRI are indicative of EPE. These include:

- **Capsular Bulging or Irregularity**:

  This is a qualitative sign seen on T2-WI, where the prostate capsule appears distorted or

pushed outward due to the pressure exerted by the underlying tumor. Capsular bulging is a well-established marker of EPE, especially when it is associated with broad tumor-capsule contact.

- **Curvilinear Contact Length (CCL)**:

  The length of contact between the tumor and the prostate capsule, as measured on axial T2-WI, is a quantitative marker of EPE. Studies have shown that a CCL greater than 15 mm is strongly associated with an increased risk of EPE. This measurement is highly reproducible across radiologists with varying levels of expertise, making it a valuable addition to EPE grading systems.

- **Capsular Breach**:

  A more definitive sign of EPE is the presence of a capsular breach, where the tumor visibly extends beyond the confines of the prostate capsule into adjacent periprostatic tissues. This is often accompanied by invasion of adjacent structures, such as the seminal vesicles or neurovascular bundles, and is a critical factor in determining surgical margins.

Challenges in Predicting EPE

A recent meta-analysis showed that both MRI-inclusive nomograms and traditonal clinical nomograsm have moderate AUCs (0.72-0.80) in EPE prediction [40]. MRI combined with clinical nomogram had higher sensitivity (0.76) compared to only MRI (0.57) [40].

Reasons for the low and variable sensitivity for EPE diagnosis may be the following. One major challenge is the variability in MRI interpretation, with outcomes highly dependent on the experience and expertise of the radiologist. Tumors located in the anterior prostate often evade detection, as the anatomy makes it harder to identify EPE. Additionally, microscopic EPE may be missed entirely due to limitations in current imaging techniques. Even though MRI-based models improve prediction accuracy, they still show false positives, making it difficult to strike a balance between sensitivity and specificity. Therefore, the need for more precise imaging protocols and standardized predictive tools that can address tumor heterogeneity and improve consistency across clinical practices are required.

Study Rationale and Objectives

Given the critical role of EPE in determining treatment outcomes in prostate cancer, there is a

pressing need for accurate, reproducible, and clinically applicable methods for preoperative EPE assessment.

This project aims at evaluating the reproducibility and predictive value of a new simplified scoring system for EPE (sEPE), based on CCL, capsular bulging/irregularity and diameter of the index lesion (diL), among readers with different level of expertise in prostate cancer imaging.

Secondly, this study aims at testing diagnostic performance sEPE grade based on tumor location the anterior versus posterior zone.

Materials and Methods

Ethics statement

This study was approved by the Institutional Review Board (AVEN 873/2018/OSS/UNIPR).

Part of the results of this study have been published [Eur Radiol. 2023 Apr;33(4):2975-2984. doi: 10.1007/s00330-022-09240-1. Epub 2022 Dec 13] and contents are reported with permission from the journal (licence ID:1541210-1).

Study Population

Consecutive patients with prostate cancer surgically treated at our University-Hospital between November 2015 and December 2018 and who underwent mpMRI within six months prior to surgery were included. The following demographic, clinical and histopathologic data were retrieved from hospital's electronic medical records: age, Prostate Specific Antigen (PSA)

values before mpMRI, type of surgical treatment (i.e., NSRP, RP or RP with lymphadenectomy), Gleason score, maximum diameter of the lesion at histology, surgical resection margins and histologic EPE. Participants selection is showed in **Figure 2.**

Figure 2. Flow-chart illustrating Participants selection.

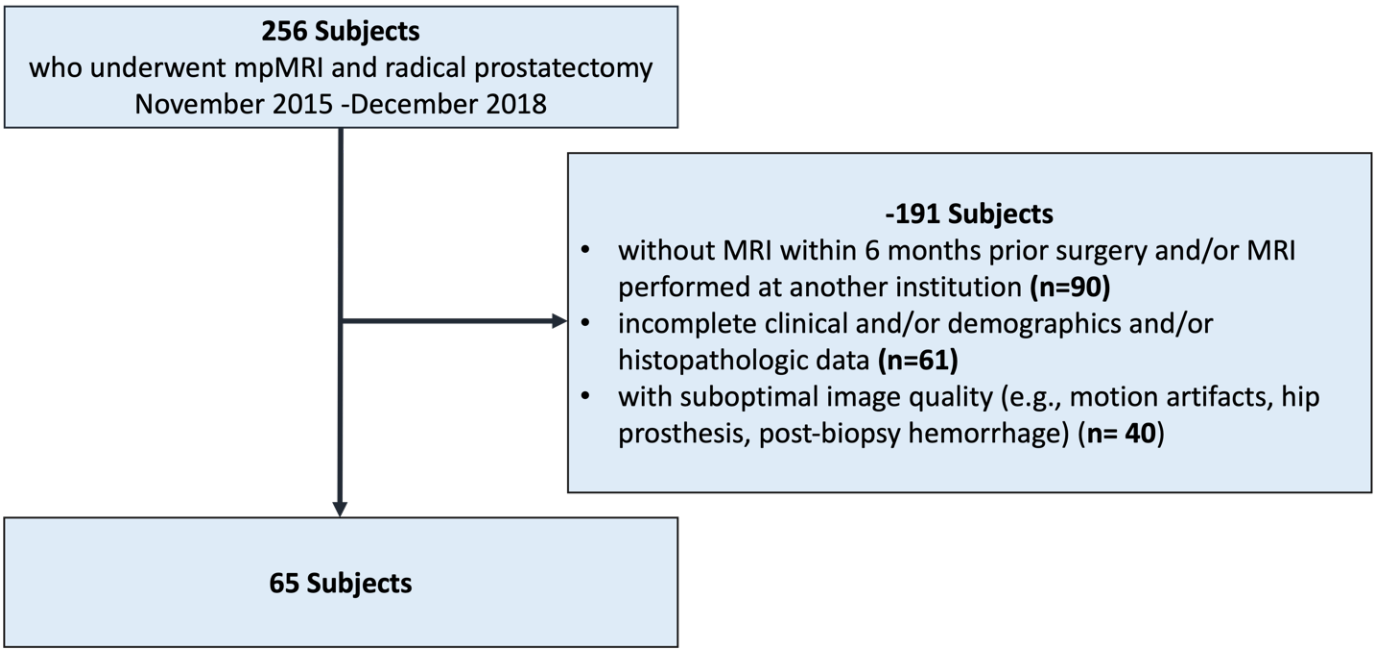

Patients risk stratification was performed according to the International Society of Urological Pathology (ISUP) classification [41] and to the D'Amico risk group score [42]. The latter system is based on PSA level, Gleason grade and T stage (size of tumor on rectal exam and/or ultrasound). D'Amico risk classification nomogram is showed in **Table 4.**

Table 4. The table shows D'Amico risk classification monogram.

Risk Class	PSA level	Gleason score	T stage
Low risk	≤10 ng/ml	≤6	T1-2a
Intermediate risk	10-20 ng/ml	7	T2b
High risk	≥20 ng/ml	≥8	T2c-3a

MRI evaluation and reporting

mpMRIs were performed by a 1.5 T MR scanner (Ingenia, Philips Healthcare, Best, Netherlands) with a 32 channels superficial phased-array coil. Technical parameters are detailed in **Table 5**.

Table 5. The Table shows technical parameters of MR Images.

Sequence description	Name	TR	TE	FA	FOV (mm)	Matrix Voxel (mm)	Slice thickness (mm)
DWI Axial, b= 50, 100, 1000, 2000 s/mm^2	SE-EPI	5011	96	90°	180x180x94	2.5x3x3.5	3.5
T2W HR Axial	SE-TSE	4716	120	90°	110x110x95	0.8x0.8x3.5	3.5
T2W HR Sagittal	SE-TSE	4379	120	90°	110x110x110	0.8x0.8x4.0	4.0
T1W Axial	SE-TSE	563	10	90°	226x323x253	1.2x1.38x6.0	6.0
3D dynamic THRIVE Axial	FFE-3D-TFE	4.0	1.9	10°	200x200x94	1.5x1.5x3.5	3.5
3D THRIVE Axial late acquisition	FFE-3D-TFE	6.2	3.0	10°	400x318x274	1.2x1.2x2.4	2.4

Readers Experience

mpMRIs were independently evaluated by seven radiologists with a different level of experience in prostate cancer imaging, ranging from 1 to 6 years. According to Puech et al. [43], readers with 2-3 years of practice in the field and 400-1200 cases read (5-15 per week) were defined as expert uroradiologist, whereas those with more than 5 years of practice in the field as highly expert uroradiologist. Therefore, readers 5-7 were considered highly expert uroradiologists and readers 1-4 expert uroradiologists. Readers were aware of the presence of underlying prostate cancer but blinded to the presence/absence of pathologic EPE.

sEPE grading system

Readers were first asked to grade images by measuring CCL, defined as the circumferential length of contact between the index lesion and the capsule obtained by means of an electronic caliper on axial T2-w image. Index lesion was defined as the lesion with the highest cancer suspicion score, regardless of its size [44]. According to Mehralivand et al. [26], a 15 mm cut-off for CCL was set as threshold for further stratification of EPE risk. Then, readers made a qualitative evaluation of "capsular bulging/irregularity" on T2-w images (**Figure 3**).

Figure 3

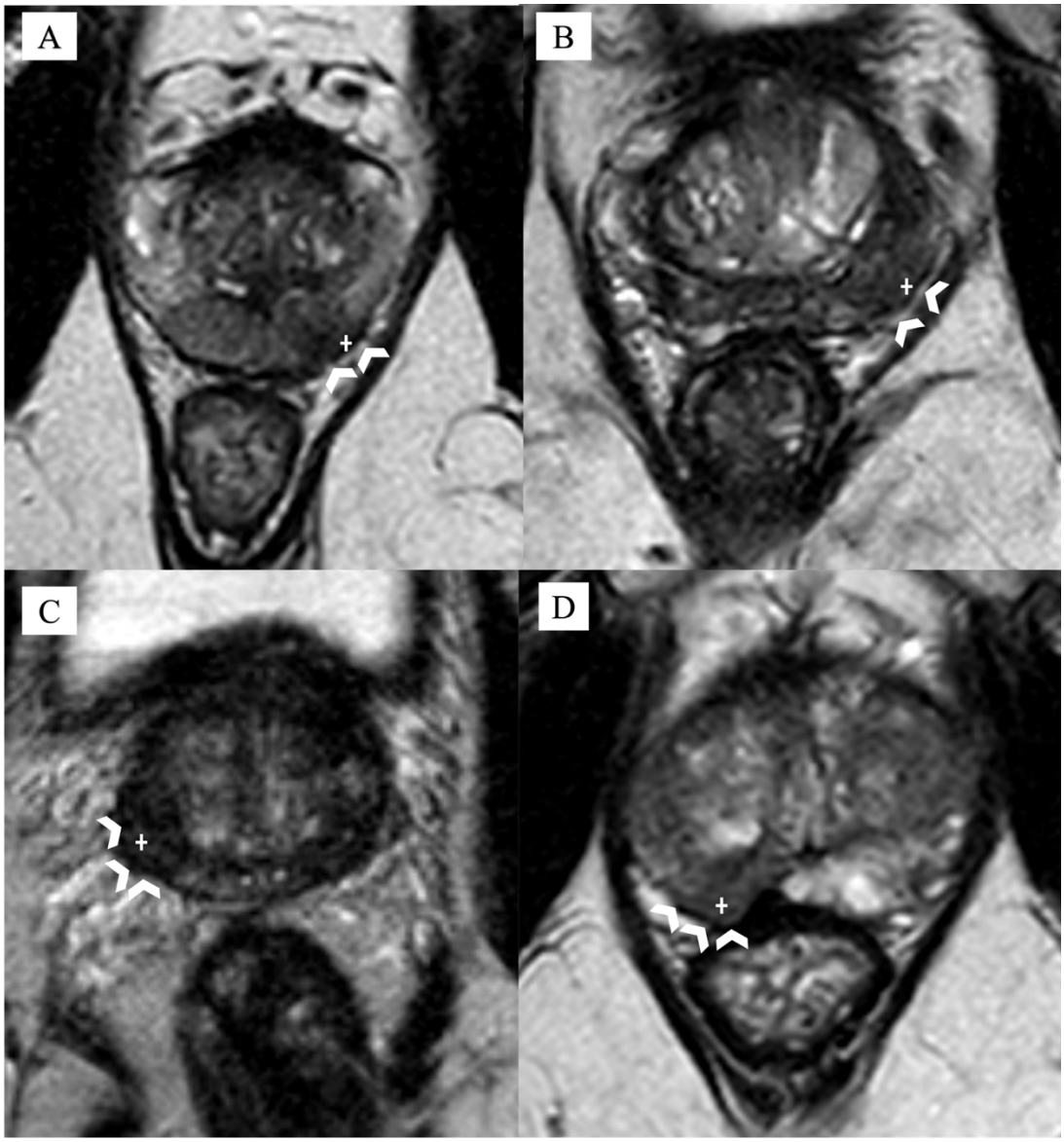

Axial T2-Weighted MR Images shows indirect capsular irregularity/bulge defined as smooth convex extension of margin prostate into extraprostatic space in continuity with intraprostatic tumor located at left posterior peripheral zone lesion (A, chevrons) and a tumor located in the left anterior peripheral zone lesion (B, chevrons); indirect curvilinear contact length defined as present when distance exceeded 15 mm associated with right posterior peripheral zone lesion (C, chevrons) and right anterior peripheral zone lesion (D, chevrons).

Readings were performed twice. At the first reading, readers were blinded to the index lesion, whereas at the second one, they all scored the same index lesion showed on a key image previously captured by the most expert reader (Reader 7) without annotated measurements. Moreover, readers reported the location of the index lesion.

Patients were subsequently classified into four categories as follows:

1) sEPE grade 0: CCL < 15 mm **without** "capsular bulging/irregularity"
2) sEPE grade 1: CCL ≥15 mm **or** "capsular bulging/irregularity"
3) sEPE grade 2: CCL≥15 mm **and** "capsular bulging/irregularity"
4) sEPE grade 3: undeniably extraprostatic tumor invasion or invasion of adjacent anatomic structures.

mpMRI maximum diameter of the index lesion

The maximum diameter of the index lesion (dIL) was measured and included in predictive models. dIL was assessed on Diffusion weighted Imaging (DWI) sequence for lesions located in the peripheral zone, and on T2-w sequence for those located in the transitional zone [27, 28].

New sEPE formulation

A new formulation of sEPE that integrates dIL* into the sEPE grade definition was proposed (**Figure 4)**. According to this new grading system, named sEPE(dIL*), patients were grouped into five categories as follows:

1) sEPE(dIL*) grade 0:
    a. CCL < 15 mm
    b. **absence of:** "capsular bulging/irregularity"
    c. dIL* < cut off
2) sEPE(dIL*) grade 1:
    a. CCL < 15 mm
    b. **absence of:** "capsular bulging/irregularity"
    c. dIL* ≥ cut off
3) sEPE(dIL*) grade 2:
    a. CCL ≥ 15 mm
    b. **presence of:** "capsular bulging/irregularity"
    c. dIL*< cut off
4) sEPE(dIL*) grade3:
    a. CCL≥ 15 mm
    b. **presence of:** "capsular bulging/irregularity"
    c. dIL* ≥ cut off
5) sEPE(dIL*) grade4: undeniably extraprostatic tumor invasion or invasion of adjacent anatomic structures.

Figure 4

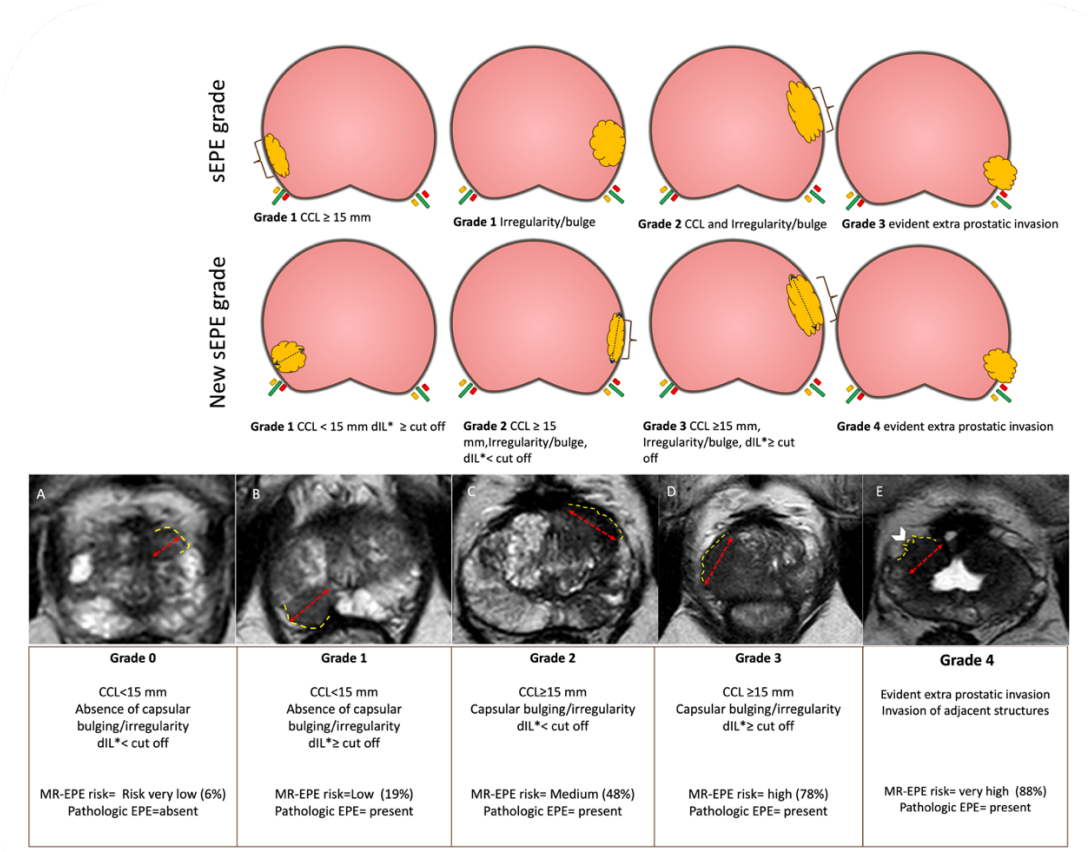

Simplified extraprostatic extension (sEPE) grading system and new sEPE grade (sEPE grade + dIL) scoring system. The sEPE grading system is a three-tier system with capsular contact length of 15 mm or greater, capsular irregularity or bulge, and frank breach of capsule: grade 0, no suspicion of pathologic EPE; grade 1, either capsular contact length (CCL) of 15 mm or greater or capsular irregularity or bulge; grade 2, both CCL 15 mm or greater and capsular irregularity or bulge; and grade 3, evident EPE invasion at MRI. The New sEPE grade scoring system consists in a new formulation of sEPE integrating dIL* into the sEPE grade definition. The new grading system, classified subjects into five categories as follows grade 0,CCL < 15 mm absence of "capsular bulging/irregularity", dIL* < cut off; grade 1,CCL < 15 mm absence of*

"capsular bulging/irregularity", dIL ≥ cut off; grade 2,CCL ≥ 15 mm and "capsular bulging/irregularity", dIL* < cut off; grade 3,CCL ≥ 15 mm and "capsular bulging/irregularity", dIL* ≥cut off; grade 4, evident EPE invasion at MRI. (A-E) Axial T2-weighted MR images show proposed the new MRI-derived simplified extraprostatic extension (sEPE) grading system for prediction of pathologic EPE (pEPE). MRI features included curvilinear contact length, defined as present when distance exceeded 15 mm (yellow dotted lines); capsular bulge, defined as smooth convex extension of margin of prostate into extraprostatic space, in continuity with intraprostatic tumor (yellow dotted lines), Diameter of the index lesion (red arrow); and EPE visible at MRI, a well-defined breach of prostate capsule with tumor extension into periprostatic space or invasion of adjacent anatomic structures (arrowhead).*

Statistical Analysis

Inter-reader agreement for CCL, presence/absence of "capsular bulging/irregularity", sEPE and dIL* was tested by weighted Cohen K coefficient (κ_w <0.20: slight; 0.21-0.40: fair; 0.41-0.60: moderate; 0.61-0.80: substantial; 0.81-1: almost perfect) and its 95% confidence interval (C.I.) [45]. The agreement for dIL before its transformation into a categorical variable (dIL*) was reported using Bland-Altman plots and Intraclass Correlation Coefficient. Youden J index was used to select the best cut-off value for dIL binarization and the resultant categorical variable was termed dIL*.

Univariable logistic regression models based on dIL*, ISUP score,

D'Amico score, sEPE and sEPE(dIL*) were developed to predict pathologic EPE. Multivariable logistic models including sEPE with one among ISUP score, D'Amico score and dIL* were also tested. Median values of sEPE, dIL and sEPE(dIL*) measurements among the three more experienced readers were used to develop the predictive models.

A nested Monte Carlo cross-validation of two loops (inner-outer) has been implemented. The outer training-validation split was iteratively repeated 100 times (with different random seeds) with a proportion of 80%-20%. For each outer training-validation split model training and validation were internally performed 100 times on training subset (80% of the whole population) with a proportion of 80%-20%. Each inner loop ended by developing a best model with tuned parameters. The dIL cut-off was determined during each outer loop on training set and subsequently applied to the validation set without modification.
The average dIL cut-off and the associated standard deviation over the 100 outer iterations were reported.

The diagnostic rate of the different EPE predictive methods was assessed in terms of accuracy, Area under the Receiver Operating Characteristics Curve (ROC-AUC), Sensitivity, Specificity, Positive Predictive Value (PPV) and Negative Predictive Value (NPV).

Final validation results were obtained averaging the performance findings over the 100 outer iterations. The most performing predictive model was further tested with the measures obtained by each one of the seven readers separately on the overall population. The likelihood-ratio (LR) test was used to compare the univariable and the multivariable models 'performances on the overall population, with sEPE grade as benchmark.

Finally, decision curve analysis was performed to estimate the benefit of each predictive model in supporting the clinical management decision-making, providing a model's description for multiple risk thresholds.

In the secondary analysis based on tumor location, we excluded four patients with an index lesion extended between anterior/posterior zone and one patient with unknown tumor location. The diagnostic rate sEPE grade in prediction based on tumor location was assessed in terms of accuracy, Area under the Receiver Operating Characteristics Curve (ROC-AUC), Sensitivity, Specificity, Positive Predictive Value (PPV) and Negative Predictive Value (NPV).

All analyses were performed with R software (version 4.0.4; www.r-project.org).

Results

Patients' characteristics according with pathologic EPE are illustrated in **Table 6**. Patients' characteristics according with tumor location are illustrated in **Table 7.**

Table 6. Patients' characteristics according with pathologic EPE

Subjects Demographic, Clinical and histopathological Characteristics	EPE - (n=34)	EPE + (n=31)	P-value
Age (y)	67.3 ± 6.4	66.6 ± 6.23	0.67 (°)
PSA (ng/mL)	7.4 ± 3.6	12.2 ± 6.9	≤0.001 (°)
Prostate volume at mpMRI (mL)	53.0 ± 28.5	43.9 ± 20.6	0.15 (°)
mpMRI dIL (mm)	13.3 ±5.6	21.6 ±6.4	≤0.001 (°)
Lesion site			0.40 (•)
Anterior	11/34 (32)	7/31 (22)	
Posterior	21/34 (62)	21/31 (68)	
Anterior/posterior	1/34 (3)	3/31 (10)	
unknown	1/34 (3)		
Systematic Biopsy	34 (100)	31 (100)	1.00
ISUP category at biopsy			
1	21 (32)	8 (28)	0.030 (•)
2	1 (2)	5 (8)	
3	6 (9)	10 (63)	
4	5 (8)	5(5)	
5	1(2)	3 (7)	
D'Amico risk group			
Low	15 (23)	4 (2)	0.020 (•)
Intermediate	11(17)	15 (58)	
High	8 (12)	12 (19)	
Type of Surgery Performed			
Nerve sparing Radical Prostatectomy	8 (12)	3 (5)	0.010 (•)
Radical Prostatectomy	11 (17)	3 (5)	
Radical Prostatectomy with lymphadenectomy	15 (23)	25 (39)	
Margins at surgery			
Negative	27 (42)	8 (12)	≤0.001 (•)
Positive	7 (11)	23 (35)	

Continuous data are expressed as mean ± SD, whereas categorical data as number with percentage in parentheses.

Table 7. Patients' characteristics according with tumor location.

	Anterior (n=18)	Posterior (n=42)	P-value
Age (y)	66.3 ±6.8	66.9 ±6.2	0.75
PSA (ng/mL)	9.3 ± 4.2	10.4 ±6.6	0.99
Prostate volume at mpMRI (mL)	44 ±16.1	46.6 ±23.6	0.99
mpMRI dIL (mm)	19.2 ±7.0	17.6 ±7.0	0.44
ISUP category at BIOPSY*			0.007 *
1	10 (55.5)	15 (36)	
2	2 (11)	4 (9.5)	
3	6 (33)	10 (24)	
4	0 (0)	8 (19)	
5	0 (0)	4 (9.5)	
unknown	0 (0)	1 (2)	
D'amico risk group			0.006*
Low	7 (39)	10 (24)	
Intermediate	10 (55.5)	15 (36)	
High	1 (5)	17 (40)	
Type of surgery performed			0.16
Nerve sparing radical prostatectomy	4 (22)	6 (14)	
Radical prostatectomy	2 (11)	11 (26)	
Radical prostatectomy with lymphadenectomy	12 (67)	25 (59)	
Margins at surgery			0.33
Negative	11 (61)	20 (48)	
Positive	7 (39)	22 (46)	
EPE at Histopathology			0.46
Negative	10 (56)	19 (45)	
Positive	8 (44)	23 (55)	

Continuous data are expressed as mean ± SD, whereas categorical data as number with percentage in parentheses.

dIL*

The optimal dIL threshold was (17.4 ± 2.7) mm, with 35 patients (53.8%) included in dIL* category 1 (i.e., with dIL > 17.4 mm).

Inter-reader Agreement

Inter-reader agreement among the seven readers is summarized in **Table 8**.

Table 8. Kw values for sEPE grade, CCL ≥15 mm, dIL* and capsular bulging/irregularity.

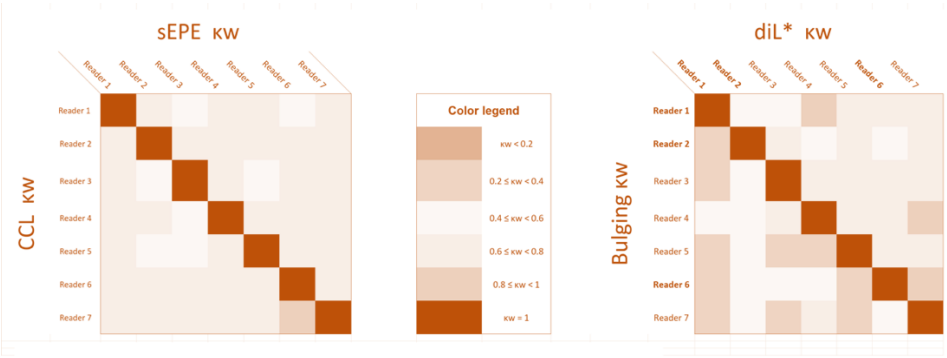

Average κ_w was 0.65 (95% C.I. 0.51,0.79), 0.66 (95% C.I. 0.48,0.84), 0.67 (95%C.I. 0.50-0.84), and 0.43 (95%C.I. 0.22-0.63) for sEPE grade, CLL ≥15 mm, dIL*, and capsular bulging/irregularity, respectively. To be noted that the agreement for dIL* measures between readers 1, 2,4 (expert uroradiologist and 6, 7 (highly expert uroradiologist) was poor even if the average agreement for dIL* was substantial (κ_w>0.6). dIL* measures of readers 2 were systematically lower than the average value of most experienced readers (**Figure 5 and Tables 9-10**).

Figure 5. Bland Altman plots for dIL* agreement

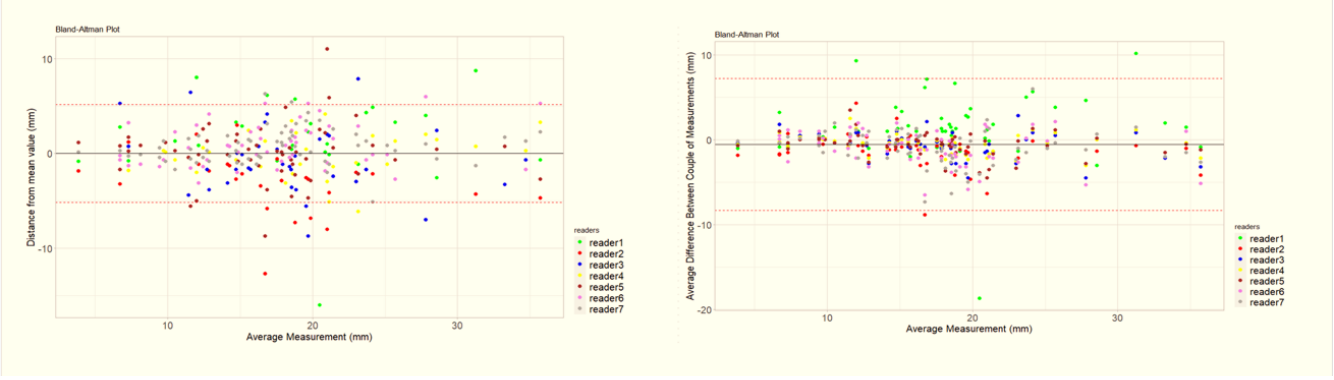

Table 9. Intraclass Correlation Coefficient for dIL agreement.

ICC		
Estimate	LowerCB	UpperCB
0.85	0.79	0.90

ICC < 0.5	Poor Reliability
0.5 <ICC ≤ 0.75	Moderate Reliability
0.75 <ICC ≤ 0.9	Good Reliability
ICC > 0.9	Excellent Reliability

Table 10. Contingency Tables for each reader

Contingency tables					
		patologic EPE		Pearson Chi-Square	p-value
		N	Y		
EPE(dIL*) : Reader1	0	26.2%	4.6%	16.5	0.002
	1	6.2%	9.2%		
	2	9.2%	7.7%		
	3	10.8%	18.5%		
	4	0.0%	7.7%		
EPE(dIL*) : Reader2	0	26.2%	6.2%	19.2	0.001
	1	1.5%	3.1%		
	2	18.5%	10.8%		
	3	4.6%	12.3%		
	4	1.5%	15.4%		
EPE(dIL*) : Reader3	0	18.5%	0.0%	18.4	0.001
	1	4.6%	6.2%		
	2	20.0%	12.3%		
	3	7.7%	18.5%		
	4	1.5%	10.8%		
EPE(dIL*) : Reader4	0	27.7%	4.6%	20.6	<0.001
	1	3.1%	4.6%		
	2	12.3%	10.8%		
	3	7.7%	13.8%		
	4	1.5%	13.8%		
EPE(dIL*) : Reader5	0	27.7%	1.5%	26.5	<0.001
	1	3.1%	4.6%		
	2	13.8%	10.8%		
	3	7.7%	18.5%		
	4	0.0%	12.3%		
EPE(dIL*) : Reader6	0	23,1%	4,6%	15.0	0.005
	1	0,0%	1,5%		
	2	10,8%	4,6%		
	3	12,3%	20,0%		
	4	6,2%	16,9%		
EPE(dIL*) : Reader7	0	24.6%	0.0%	25.2	<0.001
	1	4.6%	4.6%		
	2	10.8%	9.2%		
	3	10.8%	16.9%		
	4	1.5%	16.9%		
EPE(dIL*) : Median among high experience readers	0	26.2%	1.5%	25.1	<0.001
	1	3.1%	3.1%		
	2	15.4%	10.8%		
	3	6.2%	18.5%		
	4	1.5%	13.8%		
EPE(dIL*) : Median among high experience readers	0	20.0%	1.5%	22.7	<0.001
	1	9.2%	3.1%		
	2	12.3%	16.9%		
	3	10.8%	10.8%		
	4	0.0%	15.4%		

Association between sEPE and Pathologic EPE

Diagnostic performance of EPE Predictive Models

Both clinical (ISUP categories, D'Amico risk groups) and mpMRI (sEPE grade, dIL*) parameters predicted the presence of pathologic EPE in univariable logistic regression, with greater performance for mpMRI-derived metrics (**Table 11A**).

11A UNIVARIABLE LOGISTIC REGRESSION MODELS

	Intercept, beta	Odds Ratio (95% CI)	p-value	AIC	ROC-AUC	Accuracy	Sensitivity	Specificity	PPV	NPV
ISUP	-1.1,0.4	1.6 (1.0,2.5)	0.07	72.7	0.68	0.61	0.60	0.65	0.77	0.76
D'Amico	-1.8,0.8	2.4 (1.1,5.4)	0.05	72.0	0.67	0.57	0.77	0.37	0.72	0.78
dIL*	-3.2,2.0	7.5 (2.3,28.2)	0.003	65.9	0.73	0.73	0.67	0.78	0.72	0.78
sEPE	-1.5,1.1	3.0 (1.7,6.2)	0.001	62.9	0.77	0.67	0.74	0.59	0.83	0.84
sEPE(dIL*)	-2.4,1.0	2.8 (1.7,5.5)	<0.001	57.4	0.81	0.74	0.74	0.73	0.82	0.93

11B MULTIVARIABLE LOGISTIC REGRESSION MODELS

	Intercept, beta	Odds Ratio (95% CI)	p-value	AIC	ROC-AUC	Accuracy	Sensitivity	Specificity	PPV	NPV
ISUP	-2.1,0.3	1.4 (0.8,2.3)	0.28	63.2	0.77	0.62	0.64	0.61	0.85	0.90
sEPE	-2.1,1.0	2.8 (1.5,5.9)	0.004							
D'Amico	-2.8,0.7	2.0 (0.8,4.9)	0.17	62.4	0.77	0.62	0.62	0.62	0.85	0.90
sEPE	-2.8,1.1	2.9 (1.5,6.0)	0.004							
dIL*	-3.0,0.83	2.33 (1.2,5.1)	0.13	62.0	0.79	0.70	0.73	0.68	0.84	0.91
sEPE	-3.0,1.2	3.4 (0.8,15.0)	0.03							

sEPE model showed good sensitivity (0.74) but low specificity (0.59), while an opposite trend was observed for dIL* model. sEPE(dIL*) showed the best performance (ROC-AUC 0.81, sensitivity 0.74 and specificity 0.73) (**Figure 6**)**.**

Figure 6.

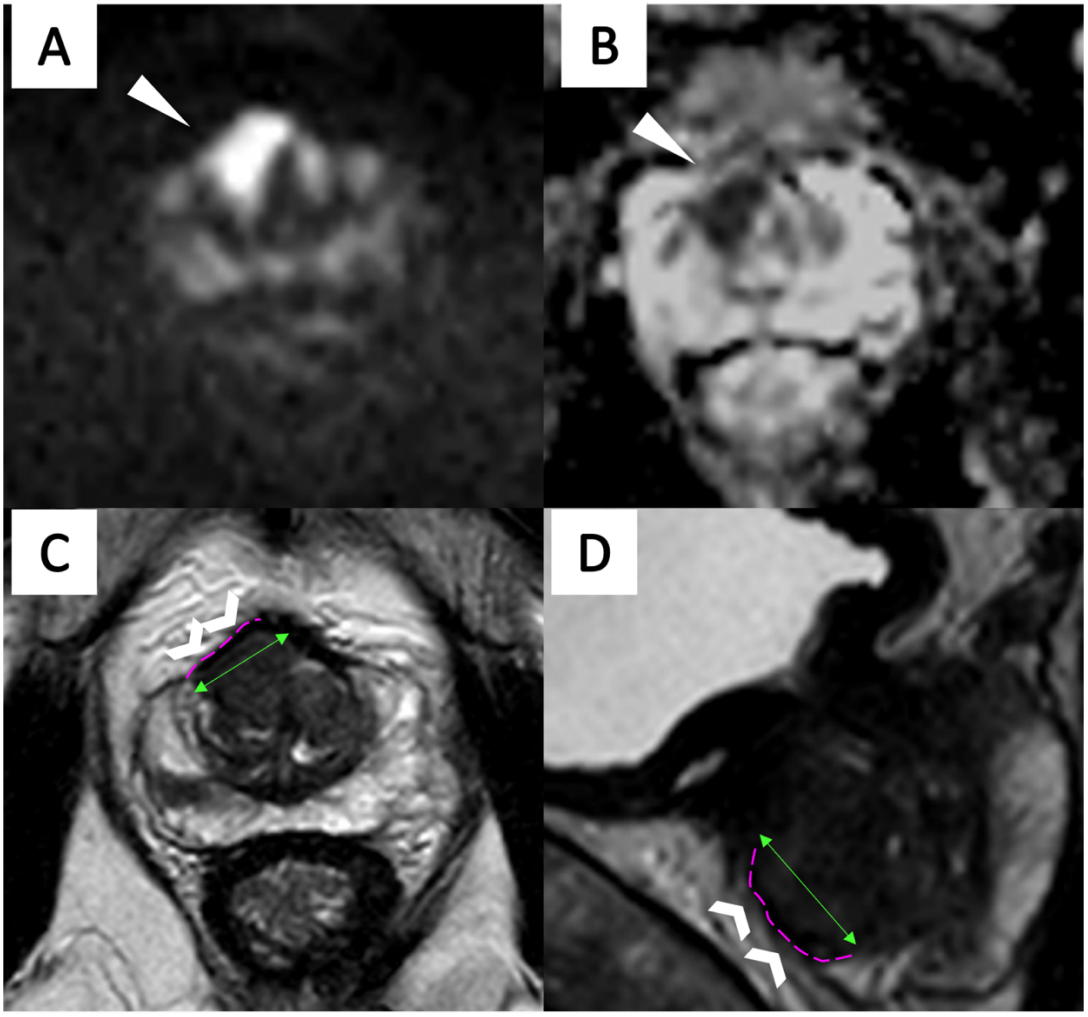

A) Axial diffusion weighted Image (DWI) showing right anterior index lesion (arrowhead) and (B) Axial Apparent Diffusion Coefficient (ADC) map of the right anterior index lesion (arrowhead);(C-D) T2 weighted axial and sagittal images showing right anterior index lesion presenting with capsular bulging and curvilinear contact length ≥15 mm (fuchsia dotted line) and subtle extraprostatic tumor extension (chevrons). The Diameter of the index lesion was above the cut-off (green arrow). The lesion was graded as 4 according to sEPE(dIL) scoring system. However, the histologic EPE was negative. This may be associated to thickness of the stromal capsule in*

the anterior region that may have acted as a barrier and may be associated with more favorable pathological characteristics of the tumor of the anterior zone.

Among the multivariable logistic regression models better performances have been observed for sEPE+dIL* (accuracy= 0.70, ROC-AUC = 0.79; **Table 11B**). The predictive performance of the models sEPE(dIL*) tested with the measures obtained by each reader showed a ROC-AUC raging between 0.75-0.89. **Figure 7** shows the comparison of ROC curves among the seven readers.

Figure 7. Roc Curves of simplified EPE

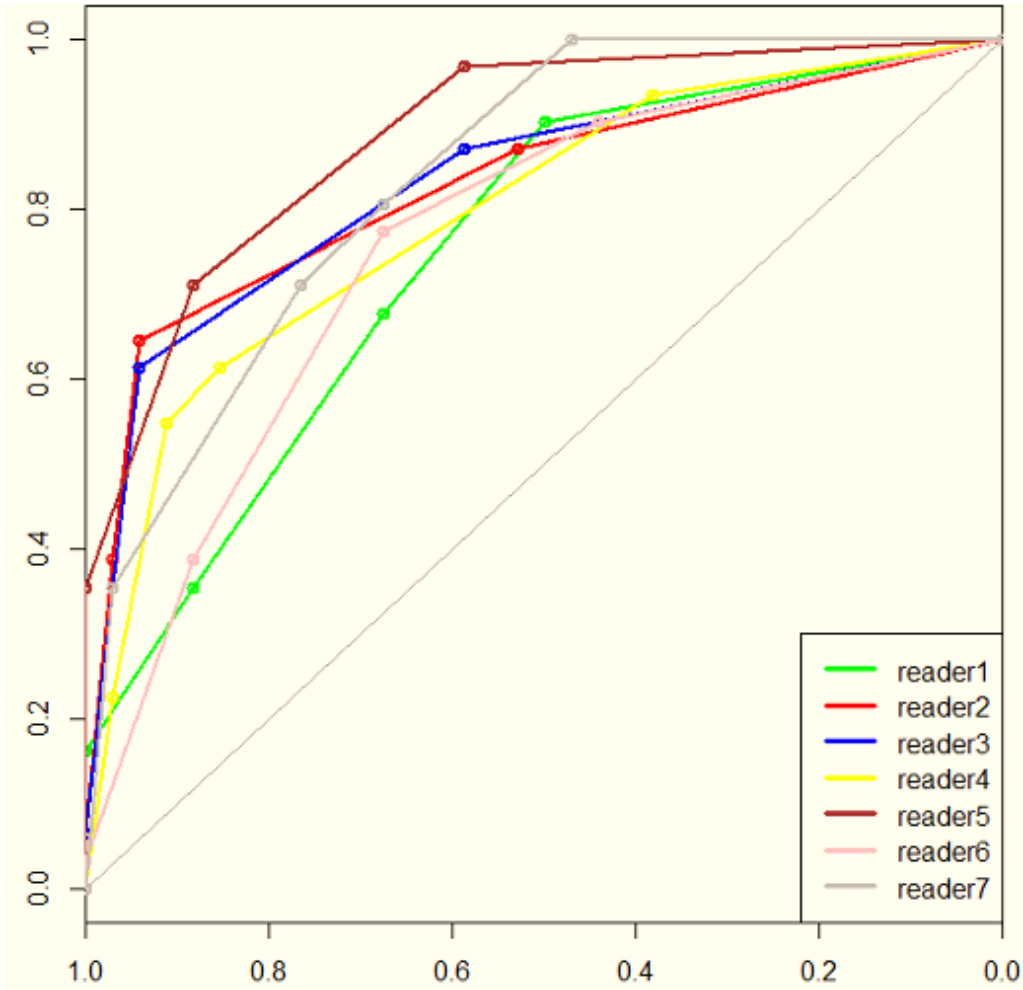

The figure shows the comparison of ROC curves of the model sEPE+dIL among the seven readers with a different level of expertise in prostate cancer imaging as follows: Readers 1-4 were expert uroradiologists (2-3 years of practice in the field) while readers 5-7 were highly expert uroradiologists (≥ 5 years of practice in the field).*

The likelihood-ratio test performed on the whole population showed an improved predictive performance by adding dIL* to sEPE grade (LR Deviance: 6.7; p = 0.01), while no

improvement was observed by adding D'Amico risk group (LR Deviance: 2.6; p = 0.10) or ISUP category (LR Deviance: 1.7; p = 0.19).

Decision Curve Analysis

As displayed in **Figure 8**, logistic models based on clinical ISUP (orange solid line), or D'Amico (brown dotted line) parameters showed higher net benefits compared to "assuming all positive" and "assuming all negative" strategies. Moreover, all mpMRI-based logistic models provided better results compared to both clinical models and simple strategies based on assumptions. Net benefit was higher for dIL* (blue dashed line) as compared to sEPE (red solid line) for central risk thresholds ranging from 0.4 to 0.7, while sEPE overcame dIL* for risk thresholds below 0.4 and above 0.7. The model sEPE(dIL*) consisting in a new sEPE formulation that include dIL* showed the best performance in the entire range of risk thresholds (green solid line).

Figure 8. Decision curve analysis

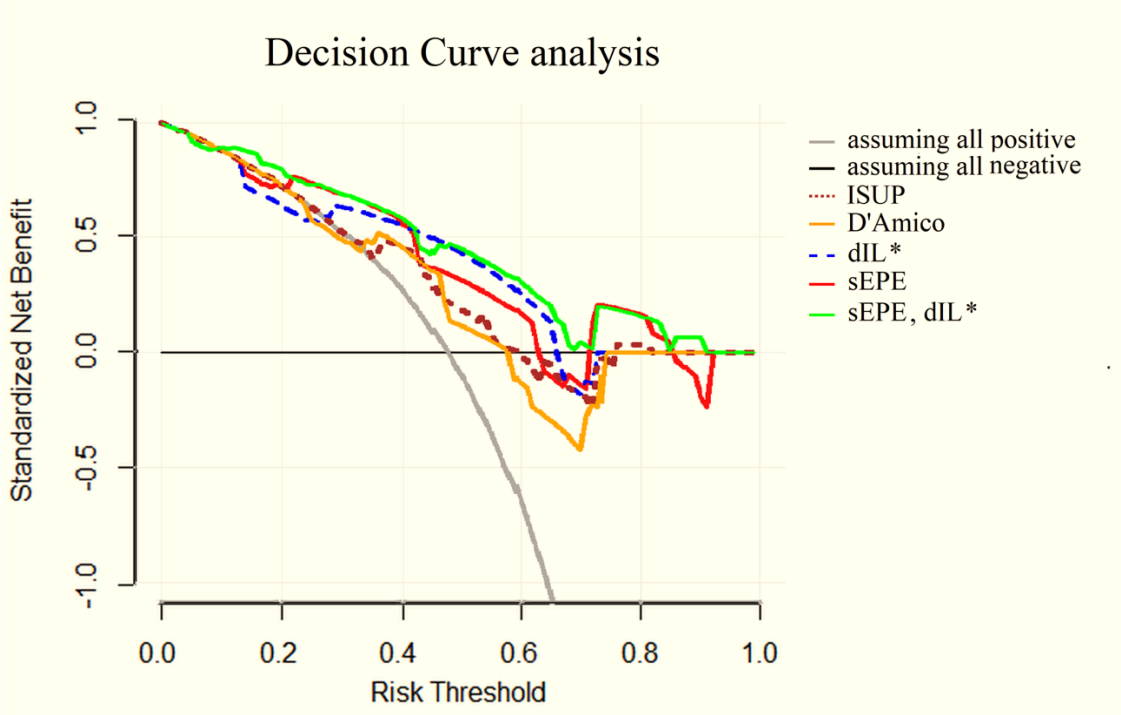

The figure shows decision curve analysis for several predictive models. The lines show the tested based mpMRI predictive models in detecting histopathological extraprostatic tumor extension. The highest net benefit was found for the model consisting in sEPE grade with dIL (green line) all risks thresholds.*

Secondary analysis based on tumor location Anterior vs posterior

EPE was found in 8/18 (44%) patients with an anterior tumor compared with 23/42 (55%) patients with a posterior tumor. The AUC was 0.88 for the anterior zone tumors and 0.77 for the posterior zone tumors. The ROC curves for sEPE of anterior or posterior tumor location are showed in **figure 9.**

Figure 9. ROC curves for sEPE based on tumor location

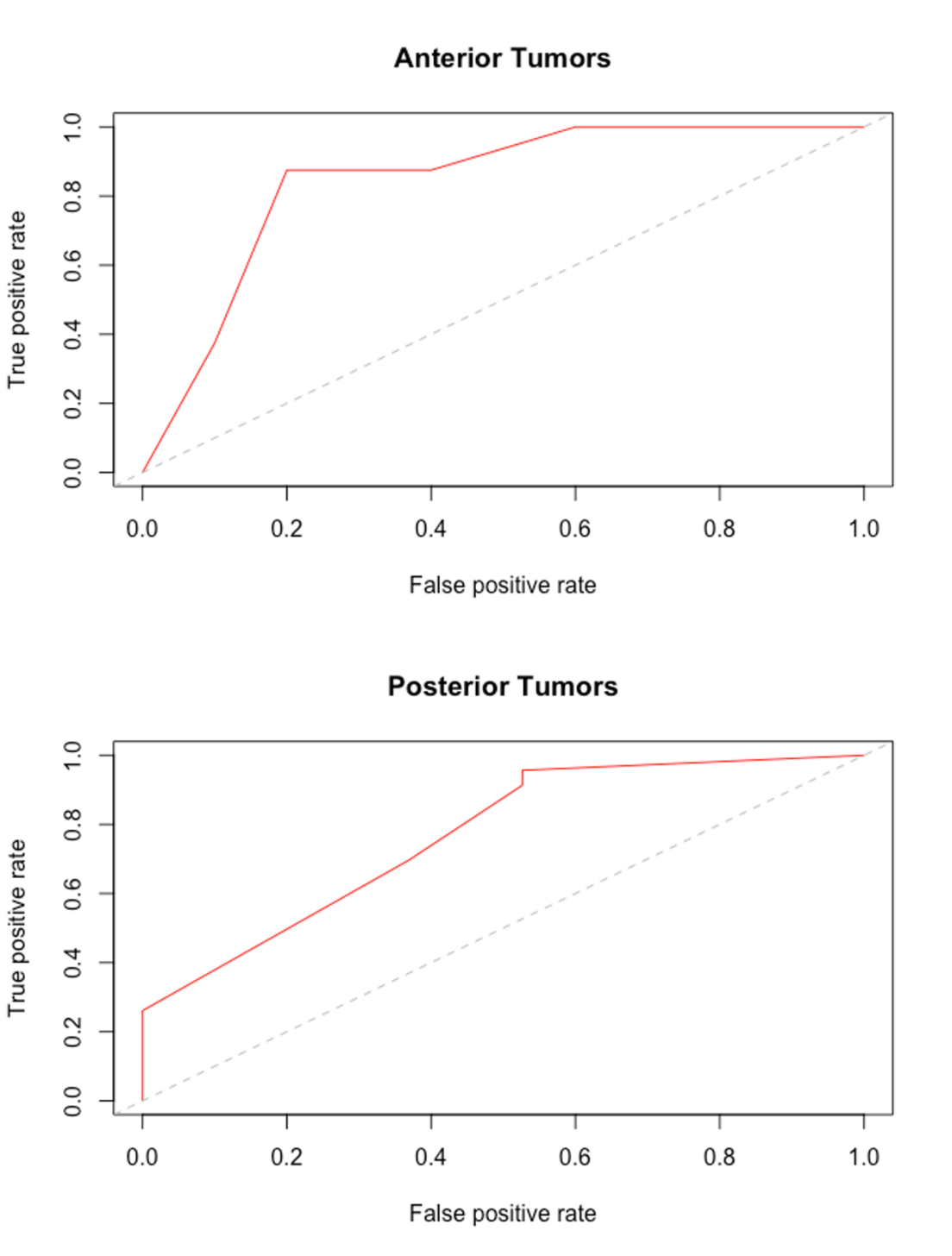

The accuracy of sEPE was of 83% in predicting extra prostatic extension on the anterior zone tumor. The accuracy of sEPE was 67% in predicting extra prostatic extension on the posterior zone tumor.

The confusion matrix of the model is shown in **Table 12** for the anterior zone and in **Table 13** for the posterior zone. Diagnostic performance of the model is shown on **Table 14.**

Table 12. Confusion matrix of the model in prediction anterior zone prostate cancer

Reference / Prediction	Negative	Positive	SUM
Negative	8 44.4%	1 5.56%	9 88.9%
Positive	2 11.1%	7 38.9%	9 77.8%
SUM	10 80.0%	8 87.5%	15/18 83.3%

Table 13. Confusion matrix of the model in prediction posterior zone prostate cancer

Reference / Prediction	Negative	Positive	SUM
Negative	12 28.6%	7 16.7%	19 63.2%
Positive	7 16.7%	16 38.1%	23 69.6%
SUM	19 63.2%	23 69.6%	28/42 66.7%

Table 14. The table shows diagnostic performance of sEPE grade based on tumor location

	Anterior zone prostate cancer	Posterior zone prostate cancer
Accuracy	0.83	0.67
Sensitivity	0.87	0.70
Specificity	0.80	0.63
PPV	0.78	0.70
PPN	0.89	0.63

Discussion

In the present study, a simplified scoring system to assess extraprostatic tumor extension (EPE) by integrating reproducible and simple qualitative and quantitative mpMRI-metrics was developed and tested. Pathologic EPE assessed after prostatectomy acted as reference standard.

EPE prediction is decisive for surgical planning as the localization and quantification of probable EPE could allow adapting the surgical approach on cancer's characteristics [46].

sEPE grade – based on evaluation of "curvilinear contact length" (CCL) and presence of "capsular bulging/irregularity" – was shown to be reproducible and to accurately predict pathologic EPE. When sEPE grade was combined with one metric detailing size of the index lesions (dIL*), the diagnostic yield for the assessment of EPE further increased.

A recent meta-analysis assessed the diagnostic performance of different EPE grading system [47]. The pooled sensitivity and specificity were 0.82 and 0.63 with an area under the ROC of 0.82. Mehralivand et al. proposed a semi-quantitative grading system with good sensitivity (80%) for EPE [26, 39], which was confirmed to correlate with histopathological extent of EPE [48]. We also included two metrics (i.e., CCL and capsular bulging/irregularity) out of the parameters of EPE grade, as they were found to display the highest reproducibility.

In this study, prostate mpMRIs were independently assessed by seven readers with a different level of experience, achieving overall good inter-reader agreement for both qualitative and quantitative parameters, in keeping with one previous study [39]. Notably, measurement of CCL was found to be of limited reproducibility by Reisaeter et al. [49] when measured by two

radiologists. In our study, conversely, the overall agreement for CCL was good (average k =0.65), even between the most and the less experienced readers.

Previous studies showed that scoring systems combining EPE grade with clinical variables were not associated with an increased diagnostic performance [48]. Similarly, in our study the combination of clinical parameters (ISUP score and D'Amico risk classification) did not improve the diagnostic performance of the mpMRI parameters alone. To further increase the diagnostic performance of our model, we tested different combination of mpMRI-features and found that the categorization of the index lesion diameter (dIL*) - when added to sEPE grade - significantly improves its predictive value (ROC-AUC of 0.86) as obtained by applying likelihood-ratio test. sEPE grade integrated with dIL* showed a good diagnostic performance even for a reader with only 2 years of experience, yielding a ROC-AUC of 0.84 thus unveiling the reproducibility of sEPE grade.

sEPE grade was validated throughout decision curve analysis, which allows to compare different predictive models and to test their impact on clinical practice [50]. Mehralivand et al. reported an increasingly higher benefit among risk thresholds greater than or equal to 20% for all models compared to the "assuming all positive" and "assuming all negative" strategies [26]. Similarly, the predictive integrated model (sEPE grade and dIL*) showed the highest net benefit for all-risk thresholds, thus potentially representing a useful decision-making tool to support clinical management, as it might allow to identify those patients who could benefit most from radical treatment. As a secondary analysis sEPE diagnostic performance was tested on tumor location. Anterior prostate cancer has been considered an indolent tumor most frequently occurring in the transition zone [51]. Detection of anterior prostate cancer has been eased by

the advent of mpMRI and improved biopsies techniques. Compared to posterior prostate cancer, anterior prostate cancers showed mean tumor volume and higher rates of positive margins. On the other hand, posterior prostate cancer showed higher grade and more frequently EPE [51]. To our knowledge, in literature very few studies discriminate separately anterior and posterior tumors and developed separate prediction for EPE [52]. It has been previously shown that anterior prostate cancers are less likely to invade the surrounding tissues compared to posterior tumors [53]. Anatomical factors contributed to this difference: the anterior fibromuscular stroma which runs horizontally and laterally at the front of the prostate, may act as a thickened capsule, providing a barrier against tumor spread. In contrast, the posterior side has periprostatic and periseminal vesicle nerves, which are more susceptible for tumor invasion. Additionally, the ejaculatory ducts, located in the central zone, may provide a pathway for posterior tumors to spread to the nearby structures like the seminal vesicles.

Ahn et al. [54] showed an AUC of 0.78 in predicting EPE of the anterior zone by evaluating only CCL. Matsumoto et al. [53] based the prediction of EPE on tumor contact length (TCL) showing a ROC of 0.89 for anterior tumors and of 0.79 for posterior tumors. However, they did not provide a cut off value for TCL. In our study, we showed similar results (ROC of 0.88 and 0.77) with a more consistent and quantitative method (CCL+ cut-off value of dIL*).

Our study suffers from several limitations. First, the retrospective design may have introduced bias selection. Second, the sample size was relatively small and further prospective multicenter studies are needed to assess sEPE grade in the clinical practice. Lastly, we did not compare sEPE grade with other MRI qualitative and quantitative methods as previous studies have shown comparable diagnostic performances.

In conclusion, the simplified EPE grading system provides a consistent and accurate assessment of pre-operative extraprostatic tumor extension, particularly for cancer located on the anterior zone.

References

[1] C.H. Pernar, E.M. Ebot, K.M. Wilson, L.A. Mucci, The Epidemiology of Prostate Cancer, Cold Spring Harb Perspect Med 8(12) (2018).

[2] C. Global Burden of Disease Cancer, C. Fitzmaurice, C. Allen, R.M. Barber, L. Barregard, Z.A. Bhutta, H. Brenner, D.J. Dicker, O. Chimed-Orchir, R. Dandona, L. Dandona, T. Fleming, M.H. Forouzanfar, J. Hancock, R.J. Hay, R. Hunter-Merrill, C. Huynh, H.D. Hosgood, C.O. Johnson, J.B. Jonas, J. Khubchandani, G.A. Kumar, M. Kutz, Q. Lan, H.J. Larson, X. Liang, S.S. Lim, A.D. Lopez, M.F. MacIntyre, L. Marczak, N. Marquez, A.H. Mokdad, C. Pinho, F. Pourmalek, J.A. Salomon, J.R. Sanabria, L. Sandar, B. Sartorius, S.M. Schwartz, K.A. Shackelford, K. Shibuya, J. Stanaway, C. Steiner, J. Sun, K. Takahashi, S.E. Vollset, T. Vos, J.A. Wagner, H. Wang, R. Westerman, H. Zeeb, L. Zoeckler, F. Abd-Allah, M.B. Ahmed, S. Alabed, N.K. Alam, S.F. Aldhahri, G. Alem, M.A. Alemayohu, R. Ali, R. Al-Raddadi, A. Amare, Y. Amoako, A. Artaman, H. Asayesh, N. Atnafu, A. Awasthi, H.B. Saleem, A. Barac, N. Bedi, I. Bensenor, A. Berhane, E. Bernabe, B. Betsu, A. Binagwaho, D. Boneya, I. Campos-Nonato, C. Castaneda-Orjuela, F. Catala-Lopez, P. Chiang, C. Chibueze, A. Chitheer, J.Y. Choi, B. Cowie, S. Damtew, J. das Neves, S. Dey, S. Dharmaratne, P. Dhillon, E. Ding, T. Driscoll, D. Ekwueme, A.Y. Endries, M. Farvid, F. Farzadfar, J. Fernandes, F. Fischer, G.H. TT, A. Gebru, S. Gopalani, A. Hailu, M. Horino, N. Horita, A. Husseini, I. Huybrechts, M. Inoue, F. Islami, M. Jakovljevic, S. James, M. Javanbakht, S.H. Jee, A. Kasaeian, M.S. Kedir, Y.S. Khader, Y.H. Khang, D. Kim, J. Leigh, S. Linn, R. Lunevicius, H.M.A. El Razek, R. Malekzadeh, D.C. Malta, W. Marcenes, D. Markos, Y.A. Melaku, K.G. Meles, W. Mendoza, D.T. Mengiste, T.J. Meretoja, T.R. Miller, K.A. Mohammad, A. Mohammadi, S. Mohammed, M. Moradi-Lakeh, G. Nagel, D. Nand, Q. Le Nguyen, S. Nolte, F.A. Ogbo, K.E. Oladimeji, E. Oren, M. Pa, E.K. Park, D.M. Pereira, D. Plass, M. Qorbani, A. Radfar, A. Rafay, M. Rahman, S.M. Rana, K. Soreide, M. Satpathy, M. Sawhney, S.G. Sepanlou, M.A. Shaikh, J. She, I. Shiue, H.R. Shore, M.G. Shrime, S. So, S. Soneji, V. Stathopoulou, K. Stroumpoulis, M.B. Sufiyan, B.L. Sykes, R. Tabares-Seisdedos, F. Tadese, B.A. Tedla, G.A. Tessema, J.S. Thakur, B.X. Tran, K.N. Ukwaja, B.S.C. Uzochukwu, V.V. Vlassov, E. Weiderpass, M. Wubshet Terefe, H.G. Yebyo, H.H. Yimam, N. Yonemoto, M.Z. Younis, C. Yu, Z. Zaidi, M.E.S. Zaki, Z.M. Zenebe, C.J.L. Murray, M. Naghavi, Global, Regional, and National Cancer Incidence, Mortality, Years of Life Lost, Years Lived With Disability, and

Disability-Adjusted Life-years for 32 Cancer Groups, 1990 to 2015: A Systematic Analysis for the Global Burden of Disease Study, JAMA Oncol 3(4) (2017) 524-548.
[3] M.S. Litwin, H.J. Tan, The Diagnosis and Treatment of Prostate Cancer: A Review, JAMA 317(24) (2017) 2532-2542.
[4] M. Sekhoacha, K. Riet, P. Motloung, L. Gumenku, A. Adegoke, S. Mashele, Prostate Cancer Review: Genetics, Diagnosis, Treatment Options, and Alternative Approaches, Molecules 27(17) (2022).
[5] M.B. Culp, I. Soerjomataram, J.A. Efstathiou, F. Bray, A. Jemal, Recent Global Patterns in Prostate Cancer Incidence and Mortality Rates, Eur Urol 77(1) (2020) 38-52.
[6] C.A. Haiman, G.K. Chen, W.J. Blot, S.S. Strom, S.I. Berndt, R.A. Kittles, B.A. Rybicki, W.B. Isaacs, S.A. Ingles, J.L. Stanford, W.R. Diver, J.S. Witte, S.J. Chanock, S. Kolb, L.B. Signorello, Y. Yamamura, C. Neslund-Dudas, M.J. Thun, A. Murphy, G. Casey, X. Sheng, P. Wan, L.C. Pooler, K.R. Monroe, K.M. Waters, L. Le Marchand, L.N. Kolonel, D.O. Stram, B.E. Henderson, Characterizing genetic risk at known prostate cancer susceptibility loci in African Americans, PLoS Genet 7(5) (2011) e1001387.
[7] K. Hemminki, K. Czene, Attributable risks of familial cancer from the Family-Cancer Database, Cancer Epidemiol Biomarkers Prev 11(12) (2002) 1638-44.
[8] E.A. Platz, E. Giovannucci, The epidemiology of sex steroid hormones and their signaling and metabolic pathways in the etiology of prostate cancer, J Steroid Biochem Mol Biol 92(4) (2004) 237-53.
[9] A.M. De Marzo, E.A. Platz, S. Sutcliffe, J. Xu, H. Gronberg, C.G. Drake, Y. Nakai, W.B. Isaacs, W.G. Nelson, Inflammation in prostate carcinogenesis, Nat Rev Cancer 7(4) (2007) 256-69.
[10] T. Pischon, H. Boeing, S. Weikert, N. Allen, T. Key, N.F. Johnsen, A. Tjonneland, M.T. Severinsen, K. Overvad, S. Rohrmann, R. Kaaks, A. Trichopoulou, G. Zoi, D. Trichopoulos, V. Pala, D. Palli, R. Tumino, C. Sacerdote, H.B. Bueno-de-Mesquita, A. May, J. Manjer, P. Wallstrom, P. Stattin, G. Hallmans, G. Buckland, N. Larranaga, M.D. Chirlaque, C. Martinez, M.L. Redondo Cornejo, E. Ardanaz, S. Bingham, K.T. Khaw, S. Rinaldi, N. Slimani, M. Jenab, E. Riboli, Body size and risk of prostate cancer in the European prospective investigation into cancer and nutrition, Cancer Epidemiol Biomarkers Prev 17(11) (2008) 3252-61.

[11] L. Zuccolo, R. Harris, D. Gunnell, S. Oliver, J.A. Lane, M. Davis, J. Donovan, D. Neal, F. Hamdy, R. Beynon, J. Savovic, R.M. Martin, Height and prostate cancer risk: a large nested case-control study (ProtecT) and meta-analysis, Cancer Epidemiol Biomarkers Prev 17(9) (2008) 2325-36.
[12] S.A. Kenfield, M.J. Stampfer, E. Giovannucci, J.M. Chan, Physical activity and survival after prostate cancer diagnosis in the health professionals follow-up study, J Clin Oncol 29(6) (2011) 726-32.
[13] N.F. Johnsen, A. Tjonneland, B.L. Thomsen, J. Christensen, S. Loft, C. Friedenreich, T.J. Key, N.E. Allen, P.H. Lahmann, L. Mejlvig, K. Overvad, R. Kaaks, S. Rohrmann, H. Boing, G. Misirli, A. Trichopoulou, D. Zylis, R. Tumino, V. Pala, H.B. Bueno-de-Mesquita, L.A. Kiemeney, L.R. Suarez, C.A. Gonzalez, M.J. Sanchez, J.M. Huerta, A.B. Gurrea, J. Manjer, E. Wirfalt, K.T. Khaw, N. Wareham, P. Boffetta, L. Egevad, S. Rinaldi, E. Riboli, Physical activity and risk of prostate cancer in the European Prospective Investigation into Cancer and Nutrition (EPIC) cohort, Int J Cancer 125(4) (2009) 902-8.
[14] A.V. Patel, C. Rodriguez, E.J. Jacobs, L. Solomon, M.J. Thun, E.E. Calle, Recreational physical activity and risk of prostate cancer in a large cohort of U.S. men, Cancer Epidemiol Biomarkers Prev 14(1) (2005) 275-9.
[15] S. Ghai, M.A. Haider, Multiparametric-MRI in diagnosis of prostate cancer, Indian J Urol 31(3) (2015) 194-201.
[16] M. de Rooij, S. Crienen, J.A. Witjes, J.O. Barentsz, M.M. Rovers, J.P. Grutters, Cost-effectiveness of magnetic resonance (MR) imaging and MR-guided targeted biopsy versus systematic transrectal ultrasound-guided biopsy in diagnosing prostate cancer: a modelling study from a health care perspective, Eur Urol 66(3) (2014) 430-6.
[17] J. Haffner, L. Lemaitre, P. Puech, G.P. Haber, X. Leroy, J.S. Jones, A. Villers, Role of magnetic resonance imaging before initial biopsy: comparison of magnetic resonance imaging-targeted and systematic biopsy for significant prostate cancer detection, BJU Int 108(8 Pt 2) (2011) E171-8.
[18] L.M. Huynh, T.E. Ahlering, Robot-Assisted Radical Prostatectomy: A Step-by-Step Guide, J Endourol 32(S1) (2018) S28-S32.

[19] N. Suardi, M. Moschini, A. Gallina, G. Gandaglia, F. Abdollah, U. Capitanio, M. Bianchi, M. Tutolo, N. Passoni, A. Salonia, P. Hedlund, P. Rigatti, F. Montorsi, A. Briganti, Nerve-sparing approach during radical prostatectomy is strongly associated with the rate of postoperative urinary continence recovery, BJU Int 111(5) (2013) 717-22.
[20] A.C. Shieh, E. Guler, V. Ojili, R.M. Paspulati, R. Elliott, N.H. Ramaiya, S.H. Tirumani, Extraprostatic extension in prostate cancer: primer for radiologists, Abdom Radiol (NY) 45(12) (2020) 4040-4051.
[21] J. Mikel Hubanks, S.A. Boorjian, I. Frank, M.T. Gettman, R. Houston Thompson, L.J. Rangel, E.J. Bergstralh, R. Jeffrey Karnes, The presence of extracapsular extension is associated with an increased risk of death from prostate cancer after radical prostatectomy for patients with seminal vesicle invasion and negative lymph nodes, Urol Oncol 32(1) (2014) 26 e1-7.
[22] O. Yossepowitch, A. Briganti, J.A. Eastham, J. Epstein, M. Graefen, R. Montironi, K. Touijer, Positive surgical margins after radical prostatectomy: a systematic review and contemporary update, Eur Urol 65(2) (2014) 303-13.
[23] A. Heidenreich, P.J. Bastian, J. Bellmunt, M. Bolla, S. Joniau, T. van der Kwast, M. Mason, V. Matveev, T. Wiegel, F. Zattoni, N. Mottet, U. European Association of, EAU guidelines on prostate cancer. part 1: screening, diagnosis, and local treatment with curative intent-update 2013, Eur Urol 65(1) (2014) 124-37.
[24] P.C. Walsh, Perfecting nerve-sparing radical prostatectomy: sailing in uncharted waters, Can J Urol 15(5) (2008) 4230-2.
[25] C. Ramsay, R. Pickard, C. Robertson, A. Close, L. Vale, N. Armstrong, D.A. Barocas, C.G. Eden, C. Fraser, T. Gurung, D. Jenkinson, X. Jia, T.B. Lam, G. Mowatt, D.E. Neal, M.C. Robinson, J. Royle, S.P. Rushton, P. Sharma, M.D. Shirley, N. Soomro, Systematic review and economic modelling of the relative clinical benefit and cost-effectiveness of laparoscopic surgery and robotic surgery for removal of the prostate in men with localised prostate cancer, Health Technol Assess 16(41) (2012) 1-313.
[26] S. Mehralivand, J.H. Shih, S. Harmon, C. Smith, J. Bloom, M. Czarniecki, S. Gold, G. Hale, K. Rayn, M.J. Merino, B.J. Wood, P.A. Pinto, P.L. Choyke, B. Turkbey, A Grading System for the

Assessment of Risk of Extraprostatic Extension of Prostate Cancer at Multiparametric MRI, Radiology 290(3) (2019) 709-719.
[27] J.C. Weinreb, J.O. Barentsz, P.L. Choyke, F. Cornud, M.A. Haider, K.J. Macura, D. Margolis, M.D. Schnall, F. Shtern, C.M. Tempany, H.C. Thoeny, S. Verma, PI-RADS Prostate Imaging - Reporting and Data System: 2015, Version 2, Eur Urol 69(1) (2016) 16-40.
[28] J.J. Futterer, M.R. Engelbrecht, H.J. Huisman, G.J. Jager, C.A. Hulsbergen-van De Kaa, J.A. Witjes, J.O. Barentsz, Staging prostate cancer with dynamic contrast-enhanced endorectal MR imaging prior to radical prostatectomy: experienced versus less experienced readers, Radiology 237(2) (2005) 541-9.
[29] M. de Rooij, E.H. Hamoen, J.A. Witjes, J.O. Barentsz, M.M. Rovers, Accuracy of Magnetic Resonance Imaging for Local Staging of Prostate Cancer: A Diagnostic Meta-analysis, Eur Urol 70(2) (2016) 233-45.
[30] D. Bonekamp, M.A. Jacobs, R. El-Khouli, D. Stoianovici, K.J. Macura, Advancements in MR imaging of the prostate: from diagnosis to interventions, Radiographics 31(3) (2011) 677-703.
[31] A. Onay, M. Vural, A. Armutlu, S. Ozel Yildiz, M.C. Kiremit, T. Esen, B. Bakir, Evaluation of the most optimal multiparametric magnetic resonance imaging sequence for determining pathological length of capsular contact, Eur J Radiol 112 (2019) 192-199.
[32] S. Woo, S.Y. Kim, J.Y. Cho, S.H. Kim, Length of capsular contact on prostate MRI as a predictor of extracapsular extension: which is the most optimal sequence?, Acta Radiol 58(4) (2017) 489-497.
[33] E. Baco, E. Rud, L. Vlatkovic, A. Svindland, H.B. Eggesbo, A.J. Hung, T. Matsugasumi, J.C. Bernhard, I.S. Gill, O. Ukimura, Predictive value of magnetic resonance imaging determined tumor contact length for extracapsular extension of prostate cancer, J Urol 193(2) (2015) 466-72.
[34] M. Kongnyuy, A. Sidana, A.K. George, A. Muthigi, A. Iyer, R. Ho, R. Chelluri, F. Mertan, T.P. Frye, D. Su, M.J. Merino, P.L. Choyke, B.J. Wood, P.A. Pinto, B. Turkbey, Tumor contact with prostate capsule on magnetic resonance imaging: A potential biomarker for staging and prognosis, Urol Oncol 35(1) (2017) 30 e1-30 e8.

[35] A.B. Rosenkrantz, A.K. Shanbhogue, A. Wang, M.X. Kong, J.S. Babb, S.S. Taneja, Length of capsular contact for diagnosing extraprostatic extension on prostate MRI: Assessment at an optimal threshold, J Magn Reson Imaging 43(4) (2016) 990-7.
[36] S. Krishna, C.S. Lim, M.D.F. McInnes, T.A. Flood, W.M. Shabana, R.S. Lim, N. Schieda, Evaluation of MRI for diagnosis of extraprostatic extension in prostate cancer, J Magn Reson Imaging 47(1) (2018) 176-185.
[37] D.N. Costa, N.M. Passoni, J.R. Leyendecker, A.D. de Leon, Y. Lotan, C.G. Roehrborn, S. Otero-Muinelo, H. Grewal, Y. Xi, F. Francis, N.M. Rofsky, I. Pedrosa, Diagnostic Utility of a Likert Scale Versus Qualitative Descriptors and Length of Capsular Contact for Determining Extraprostatic Tumor Extension at Multiparametric Prostate MRI, AJR Am J Roentgenol 210(5) (2018) 1066-1072.
[38] R.V. Chandra, S. Heinze, R. Dowling, C. Shadbolt, A. Costello, J. Pedersen, Endorectal magnetic resonance imaging staging of prostate cancer, ANZ J Surg 77(10) (2007) 860-5.
[39] K.J. Park, M.H. Kim, J.K. Kim, Extraprostatic Tumor Extension: Comparison of Preoperative Multiparametric MRI Criteria and Histopathologic Correlation after Radical Prostatectomy, Radiology 296(1) (2020) 87-95.
[40] M. Zhu, J. Gao, F. Han, L. Yin, L. Zhang, Y. Yang, J. Zhang, Diagnostic performance of prediction models for extraprostatic extension in prostate cancer: a systematic review and meta-analysis, Insights Imaging 14(1) (2023) 140.
[41] L. Egevad, B. Delahunt, J.R. Srigley, H. Samaratunga, International Society of Urological Pathology (ISUP) grading of prostate cancer - An ISUP consensus on contemporary grading, APMIS 124(6) (2016) 433-5.
[42] D.J. Hernandez, M.E. Nielsen, M. Han, A.W. Partin, Contemporary evaluation of the D'amico risk classification of prostate cancer, Urology 70(5) (2007) 931-5.
[43] P. Puech, M. Randazzo, A. Ouzzane, V. Gaillard, A. Rastinehad, L. Lemaitre, A. Villers, How are we going to train a generation of radiologists (and urologists) to read prostate MRI?, Curr Opin Urol 25(6) (2015) 522-35.
[44] S. Rais-Bahrami, B. Turkbey, A.R. Rastinehad, A. Walton-Diaz, A.N. Hoang, M.M. Siddiqui, L. Stamatakis, H. Truong, J.W. Nix, S. Vourganti, K.B. Grant, M.J. Merino, P.L. Choyke, P.A. Pinto,

Natural history of small index lesions suspicious for prostate cancer on multiparametric MRI: recommendations for interval imaging follow-up, Diagn Interv Radiol 20(4) (2014) 293-8.
[45] J.R. Landis, G.G. Koch, An application of hierarchical kappa-type statistics in the assessment of majority agreement among multiple observers, Biometrics 33(2) (1977) 363-74.
[46] B. Rocco, M.C. Sighinolfi, M. Sandri, A. Eissa, A. Elsherbiny, A. Zoeir, H. Tadzia, H. Palayapalayam, D. Kameh, R. Coelho, S. Puliatti, P. Zuccolotto, R. Montironi, P. Wiklund, S. Micali, G. Bianchi, V. Patel, Is Extraprostatic Extension of Cancer Predictable? A Review of Predictive Tools and an External Validation Based on a Large and a Single Center Cohort of Prostate Cancer Patients, Urology 129 (2019) 8-20.
[47] W. Li, W. Shang, F. Lu, Y. Sun, J. Tian, Y. Wu, A. Dong, Diagnostic Performance of Extraprostatic Extension Grading System for Detection of Extraprostatic Extension in Prostate Cancer: A Diagnostic Systematic Review and Meta-Analysis, Front Oncol 11 (2021) 792120.
[48] L. Xu, G. Zhang, X. Zhang, X. Bai, W. Yan, Y. Xiao, H. Sun, Z. Jin, External Validation of the Extraprostatic Extension Grade on MRI and Its Incremental Value to Clinical Models for Assessing Extraprostatic Cancer, Front Oncol 11 (2021) 655093.
[49] L.A.R. Reisaeter, O.J. Halvorsen, C. Beisland, A. Honore, K. Gravdal, A. Losnegard, J. Monssen, L.A. Akslen, M. Biermann, Assessing Extraprostatic Extension with Multiparametric MRI of the Prostate: Mehralivand Extraprostatic Extension Grade or Extraprostatic Extension Likert Scale?, Radiol Imaging Cancer 2(1) (2020) e190071.
[50] L. Wynants, M. van Smeden, D.J. McLernon, D. Timmerman, E.W. Steyerberg, B. Van Calster, t. Topic Group 'Evaluating diagnostic, S.i. prediction models' of the, Three myths about risk thresholds for prediction models, BMC Med 17(1) (2019) 192.
[51] H. Samaratunga, L. Egevad, J.W. Yaxley, S. Johannsen, I.K. Le Fevre, J.L. Perry-Keene, T. Gianduzzo, C. Chabert, G. Coughlin, R. Parkinson, B. Kua, W. Yaxley, B. Delahunt, Clinicopathologic Significance of Anterior Prostate Cancer: Comparison With Posterior Prostate Cancer in the Era of Multiparametric Magnetic Resonance Imaging, Am J Surg Pathol 47(6) (2023) 701-708.

[52] E. Rud, L. Diep, E. Baco, A prospective study evaluating indirect MRI-signs for the prediction of extraprostatic disease in patients with prostate cancer: tumor volume, tumor contact length and tumor apparent diffusion coefficient, World J Urol 36(4) (2018) 629-637.
[53] K. Matsumoto, H. Akita, K. Narita, A. Hashiguchi, K. Takamatsu, T. Takeda, T. Kosaka, R. Mizuno, E. Kikuchi, M. Oya, M. Jinzaki, Prediction of extraprostatic extension by MRI tumor contact length: difference between anterior and posterior prostate cancer, Prostate Cancer Prostatic Dis 22(4) (2019) 539-545.
[54] H. Ahn, S.I. Hwang, H.J. Lee, H.S. Suh, G. Choe, S.S. Byun, S.K. Hong, S. Lee, J. Lee, Prediction of extraprostatic extension on multi-parametric magnetic resonance imaging in patients with anterior prostate cancer, Eur Radiol 30(1) (2020) 26-37.